Structural and magnetic properties of polynuclear oximate copper complexes with different topologies

Structural and Magnetic Properties of New Polynuclear Oximate Copper Complexes

Lorena Martínez [a], Carla Bazzicalupi [b], Antonio Bianchi [b], Francesc Lloret [c], Ricardo González [a], Carlos Kremer [a], Raúl Chiozzone [a,*]

[a] Área Química Inorgánica, DEC, Facultad de Química, Universidad de la República, Montevideo, Uruguay

[b] Dipartimento di Chimica, Università degli Studi di Firenze, Sesto Fiorentino, Italy

[c] Departament de Química Inorgánica/Instituto de Ciencia Molecular, Facultat de Química de la Universitat de València, València, Spain

Abstract

Two new copper(II) complexes containing the methyl(2-pyridyl)ketone oxime ligand (mpkoH) $[Cu_3(OH)(ClO_4)_2(mpko)_3]\cdot CH_3OH$ (**1**) and $[Cu(ClO_4)(mpko)(mpkoH)]_n$ (**2**) have been prepared from $Cu(ClO_4)_2$ and mpkoH in different metal-to-ligand molar ratios. In addition, the compound $\{Cu[(mpko)_2BF_2](H_2O)\}BF_4$ (**3**) $[(mpko)_2BF_2$ is the fluoroboration product of the oxime] has been obtained when replacing $Cu(BF_4)_2$ by $Cu(ClO_4)_2$. Compound **1** is an isolated triangle with a $[Cu_3(\mu_3\text{-}OH)]$ core, whereas **2** ~~is~~ a chain of Cu^{II} ions linked by anionic $mpko^-$ bridges. **1** exhibits strong antiferromagnetic competing interactions, as well as antisymmetric exchange. On the other hand, very weak ferromagnetic interactions are found in **2**. The magnetic properties of these compounds have been analyzed by susceptibility and EPR measurements.

Keywords

Copper(II) complexes, methyl(2-pyridyl)ketone oxime, magnetic properties

1. Introduction

2-Pyridyl oximes, of general formula (py)(R)C=NOH with py = pyridine and R = H, alkyl or aryl group, have been known for a long time as spectrophotometric reagents in analytical chemistry [1]. More recently, they became very popular ligands in molecular magnetism, due mainly to their ability to form polynuclear complexes by acting as versatile and flexible bridging ligands that efficiently mediate magnetic exchange between paramagnetic ions [2].

Many complexes of first transition metals and/or lanthanide ions with 2-pyridyl oximes have been characterized and their magnetic properties investigated in the last years [3–15]. Some outstanding examples are the trinuclears $[Mn^{III}_3O(O_2CR)_3(mpko)_3](ClO_4)$ ($mpko^-$ = methyl(2-pyridyl)ketone oximate, R = Me, Et, Ph) [16] and the 3d/5f spin cluster $[Ni_8Dy_8O(OH)_4(pao)_{28}](ClO_4)_5(NO_3)$ (pao^- = 2-pyridinealdoximate) [17] which behave as single-molecule magnets, or $[Mn_2(saltmen)_2Ni(pao)_2(py)_2](ClO_4)_2$ ($saltmen^{2-}$ = N,N-(1,1,2,2-tetramethylethylene) bis(salicylideneiminate) which was the first heterometallic single-chain magnet [18].

Several copper(II) complexes with this kind of ligands have also been reported, mainly with phenyl(2-pyridyl)ketone oxime (ppkoH), bis(2-pyridyl)ketone oxime (dpkoH) or 2-pyridinealdoxime, and mostly di- or trinuclear compounds [19–30]. $[Cu_3(OH)(6\text{-}mepao)_3(O_2CPh)_2]$ (6-$mepao^-$ = 6-methyl-2-pyridylaldoximate) [31] and $[Cu_3(OH)(Br)(ppko)_3(^tBuPO_3H)(MeOH)]\cdot 1.5\ MeOH$ [32] are recent representative examples of a triangular motif that leads to spin-frustrated systems and has been found to resemble the active site of multicopper oxidases enzimes [33]. The $\{Cu_3(\mu_3\text{-}OR)(oximate)_3\}^{n+}$ core can also be recognized in discrete hexanuclear copper(II) cages [31] and in one-dimensional coordination polymers as $[Cu_3(OH)(ppko)_3(N(CN)_2)(O_2CMe)]_n$ or $\{[Cu_3(OH)(pao)_3(bdc)]\cdot 6H_2O\}_n$ (bdc^{2-} = benzene-1,4-dicarboxylate), where the trinuclear cores are bridged by dicyanamide or bis-carboxylato linkers, respectively [34,35].

By contrast, as far as we know, up to November 2016 only two Cu^{II} complexes with the ligand methyl(2-pyridyl)ketone oxime (Scheme 1), the mononuclears $[Cu(mpko)Cl(mpkoH)]\cdot 3H_2O$ [36] and $[Cu(mpko)(mpkoH)(H_2O)]ClO_4\cdot H_2O$ [37], had been crystallographically characterized. In this work, we report the synthesis and crystal structure of three new copper complexes with mpkoH, namely $[Cu_3(OH)(ClO_4)_2(mpko)_3]\cdot CH_3OH$ (**1**), $[Cu(ClO_4)(mpko)(mpkoH)]_n$ (**2**) and $\{Cu[(mpko)_2BF_2](H_2O)\}BF_4$ [$(mpko)_2BF_2^-$ = difluoro-bis[[(*E*)-1-(2-pyridyl)ethylideneamino]oxy]boranuide] (**3**). Compound **1** is an isolated μ_3-OH-bridged copper triangle, **2** is a novel 1D chain compound and **3** is a mononuclear complex. The magnetic properties of **1** and **2** have been studied in detail by means of susceptibility, magnetization and EPR measurements.

2. Experimental

2.1. General procedures

The ligand mpkoH was prepared from 2-acetylpyridine and hydroxylamine following the literature procedure reported by Chaudhuri [38]. All other reagents and solvents were purchased from commercial sources and ~~were~~ used as received.

Safety Note: The perchlorate salts of complexes with organic ligands are potentially explosive. We worked on the mmol scale and any heating was avoided. Efforts to replace the perchlorate anions by other non-coordinating friendly anions such as triflate or tetrafluoroborate are recommended.

Infrared spectra were recorded with a Shimadzu IRPrestige-21 FTIR spectrometer as KBr pellets in the 4000–400 cm^{-1} region. Elemental analyses for carbon, hydrogen and nitrogen were performed on a Thermo Flash 2000 analyzer. X-band EPR spectra of polycrystalline samples were recorded at different temperatures with a Bruker ER 200 spectrometer equipped with a helium continuous-flow cryostat. Variable-temperature magnetic susceptibility measurements were carried out on polycrystalline samples using a Cryogenics SX600 SQUID magnetometer in the temperature range of 1.9–300 K under an applied magnetic field of 10000 Oe at high temperatures and of 1000 Oe below 40 K to avoid magnetic saturation. The device was calibrated with YFe garnet NIST reference samples. Diamagnetic corrections of the constituent atoms were estimated from Pascal's constants. Experimental susceptibilities were also corrected for the temperature-independent paramagnetism [60×10^{-6} cm^3 mol^{-1} per copper(II)] and for the magnetization of the sample holder.

*2.2. Synthesis of [Cu_3(μ-mpko)$_3$(μ_3-OH)(μ_3-ClO_4)(ClO_4)]·CH_3OH (**1**)*

Solid mpkoH (0,5 mmol, 68 mg) was added to a solution of $Cu(ClO_4)_2\cdot 6H_2O$ (0,5 mmol, 185 mg) in CH_3OH (10 mL) and stirred at room temperature during 15 minutes. Then, NaOH (0,5 mmol, 20 mg) was added to the dark-green solution. A green precipitate of **1** was filtered off washed with cold CH_3OH and air-dried. The filtrate solution was allowed to evaporate very slowly, and a second crop of crystals was obtained after one week. Yield: 60 %. Green prisms of **1** suitable for X-ray diffraction studies were obtained directly from the mother liquor. Selected IR bands

[ν_{max}/cm^{-1}]: 3422br, 3099w, 2360w, 2343w, 1603s, 1551m, 1474s, 1422w, 1377w, 1339w, 1267w, 1161s, 1121s, 1109s, 1086s, 1049s, 930w, 820w, 783m, 703m, 657w, 624m, 508w, 488m, 409w. *Anal*. Calc. for $Cu_3C_{22}H_{26}N_6O_{13}Cl_2$: C, 31.31; H, 3.10; N, 9.96. Found: C, 30.94; H, 3.08; N, 9.93%.

*2.3. Synthesis of [Cu(ClO$_4$)(μ-mpko)(mpkoH)]$_n$ (**2**)*

Solid mpkoH (1 mmol, 136 mg) was added to a solution of $Cu(ClO_4)_2 \cdot 6H_2O$ (0,5 mmol, 185 mg) in CH_3OH (10 mL) and stirred at room temperature during 15 minutes. The dark-green solution was allowed to evaporate very slowly. ~~After one week, red-brown crystals were formed~~, filtered, washed with cold CH_3OH and air-dried. Yield: 15 %. Prisms of **2** ~~suitable for~~ X-ray diffraction studies were obtained directly from the mother liquor. Selected IR bands [ν_{max}/cm^{-1}]: 3452br, 1604m, 1562m, 1481m, 1350w, 1165m, 1111s, 1091s, 1023w, 783m, 702w, 621m. *Anal*. Calc. for $CuC_{14}H_{15}N_4O_6Cl$: C, 38.72; H, 3.48; N, 12.90. Found: C, 38.25; H, 4.41; N, 12.41%.

*2.4. Synthesis of {Cu[(mpko)$_2$BF$_2$](H$_2$O)}BF$_4$ (**3**)*

Solid mpkoH (1 mmol, 136 mg) was added to a solution of $Cu(BF_4)_2 \cdot 6H_2O$ (0,5 mmol, 200 mg) in H_2O (7 mL) while stirring at room temperature. The dark-green solution was allowed to evaporate very slowly and after one week, a green crystalline solid was formed, filtered, washed with CH_3OH:H_2O (1:1) and air-dried. Yield: 45 %. Green prisms of **3** suitable for X-ray diffraction studies were obtained directly from the mother liquor. Selected IR bands [ν_{max}/cm^{-1}]: 3630m, 3620m, 3555m, 3476m, 1636w, 1616m, 1601m, 1564w, 1485m, 1445w, 1383s, 1344m, 1261w, 1196m, 1167s, 1146s, 1107s, 1092s, 1072s, 1051s, 1034s, 968s, 895m, 864w, 781s, 746w, 692m, 638w, 606w, 565w, 532m, 521m, 422w. *Anal*. Calc. for $CuB_2C_{14}H_{16}N_4O_3F_6$: C, 34.50; H, 3.31; N, 11.49. Found: C, 33.75; H, 3.44; N, 11.69 %.

2.5. X-ray Data Collection and Structure Refinement

$C_{22}H_{26}Cl_2Cu_3N_6O_{13}$; MW = 844.01; a = 9.1718(3) Å, b = 17.1060(6) Å, c = 19.1714(7) Å, β = 92.257(4)°, V = 3005.5(2) Å^3, monoclinic, $P2_1/c$, Z = 4, approximate crystal dimensions 0.3x0.2x0.1 mm^{-1}, ρ_{calcd} = 1.865 mg/cm^3, Cu-kα radiation (λ = 1.54180 Å), μ = 4.775 mm^{-1}, ω-scan, T = 150 K, 13591 reflections collected up to θmax = 71.17°, 5665 independent reflections (R_{int} = 0.0585), final agreement factors R1 = 0.0702 and wR2 = 0.1634 for 395 refined parameters and 3870 independent reflections with I > 2σ(I), R1 = 0.1084 and wR2 = 0.1845 for all the 5665 independent reflections.

A green crystal of **1** was used for X-ray diffraction analysis. The integrated intensities were corrected for Lorentz and polarization effects and an empirical absorption correction was applied (T_{min} = 0.69235, T_{max} = 1.00000 -CrysAlisPro, Agilent Technologies, Version 1.171.35.11). The structure was solved by Patterson method (SHELXS-86). (Sheldrick, G. M. *Acta. Cryst.* **1990**, *A46*, 467–473) Refinements were performed by means of full-matrix least-squares using SHELXL-97 program. (G. M. Sheldrick, *Acta Cryst. A*, 2008, **64**, 112-122) All the non-hydrogen atoms were anisotropically refined, while all the hydrogen atoms were introduced using a riding model and their coordinates were refined according to the linked atoms. The only exception was the hydrogen atom belonging to the bridging hydroxide, which was located in the Fourier difference map, and freely refined with isotropic ADP. CIF file is available from the Cambridge Crystallographic Data Center (CCDC number 864757).

Single-crystal X-ray diffraction experiments on **3** were performed with a Bruker D8 Venture diffractometer operating with a sealed-tube Mo Kα radiation (λ = 0,71069 Å) and a PHOTON100 CMOS area detector, at room temperature.
Crystal data, collection procedures and refinement results are summarized in Table 1.

3. Results and discussion

3.1. Synthesis

The reaction between $Cu(ClO_4)_2$ and mpkoH in equimolar ratio in CH_3OH leads to formation of the trinuclear compound **1** containing the $\{Cu_3(\mu_3\text{-}OH)\}^{5+}$ core, as summarized in Eq. 1. The addition of base is not required ~~for the obtention of~~ **1**, but it promotes the deprotonation of the oxime, thus improving yields.

$3Cu^{2+} + 3mpkoH + 3OH^- + 2ClO_4^- \rightarrow [Cu_3(OH)(ClO_4)_2(mpko)_3] + H_3O^+ + H_2O$ (1)

Complex formation depends on the metal-to-ligand reaction ratio. So, when the Cu^{II}:mpkoH molar ratio is changed to 1:2 compound **2** is obtained (Eq. 2).

$Cu^{2+} + 2mpkoH + ClO_4^- \rightarrow [Cu(ClO_4)(mpko)(mpkoH)] + H^+$ (2)

Unfortunately, all attempts to resolve the crystal structure of **2** were unsuccessful owing to serious pseudosymmetry problems related to disordered perchlorate anions (see caption to Figure Sx). Nevertheless, the obtained structural model is sufficiently clear, allowing us to propose for **2** the chain structure shown in Figure Sx. As far as we know, this would be the first example of a 2-pyridyl oximate-bridged homonuclear Cu^{II} chain.

~~Due to the disorder revealed in the crystal structure of **2**~~, we attempted the preparation of the analogous BF_4^- chain by employing $Cu(BF_4)_2$ instead of $Cu(ClO_4)_2$. This approach, however, was unsuccessful, an the only isolated product in this case was the mononuclear complex **3**. The tetradentate ligand $(mpko)_2BF_2^-$ was formed *in situ* by the copper(II)-assisted fluoroboration of the oxime with BF_4^-. The reaction described in Eq. 3 takes place in CH_3OH, although higher yields for the synthesis of **3** were attained in aqueous media.

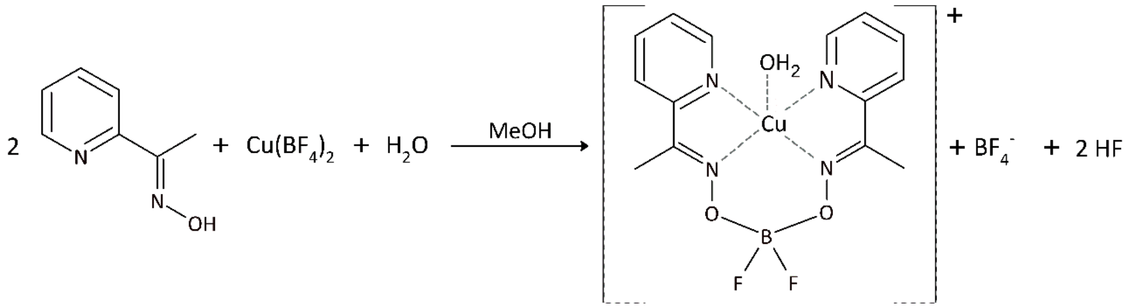

(3)

3.2. Description of the structures

Perspective drawings of the structures of compounds **1**–**3** showing the relevant atom numbering scheme are depicted in Figures 1–3, respectively. Selected bond lengths and angles are listed in Tables 2, 4 and 5.

Compound **1** crystallizes in the centrosymmetric monoclinic space group $P2_1/c$. Its structure consist of neutral $\{Cu_3\}$ trinuclear units and methanol molecules of crystallization. In the $[Cu_3(mpko)_3(\mu_3\text{-}OH)(ClO_4)_2]$ unit, the three copper atoms are located at the corners of a nearly equilateral triangle that is kept together by three $mpko^-$ ligands bridging pairs of copper atoms along the edges of the triangle (in a 2.111 mode according to Harris notation [39] (see Scheme 1)), a triply bridging hydroxide ion on one side of the triangle and a perchlorate anion bridging the three copper atoms in a 3.1110 mode on the other side. The Cu···Cu distance in the trinuclear unit ranges from 3.203(2) to 3.225(2) Å. The O(41) from the μ_3-OH ion is located 0,568(5) Å out of the plane of the triangle, and the Cu–O(41)–Cu angles range from 111.1(2) to 112.5(3)°. The two N atoms from each $mpko^-$ ligand are both coordinated to one metal atom forming a five-membered chelate ring, while the O atom of the oximate group is bound to the neighboring copper atom in *syn* conformation. In turn, Cu–N–O–Cu dihedral angles average 9.4(6)°. This way, the coordination around Cu(1) and Cu(2) is square pyramidal, with a N_2O_3 environment defined by the two N atoms from one $mpko^-$ ligand, one O atom from the oximato bridge, one O atom from the μ_3-OH and one O from the ClO_4^- ion in the apical position. The second perchlorate anion is bound to the remaining copper atom in an asymmetric monodentate way, occupying the second elongated axial position in a rather distorted N_2O_4 octahedron around Cu(3). Cu–N distances average 1.966(6) Å, and their values are in the range found for similar compounds [22]. The Cu–O(ClO_4^-) distances are larger [2.422(6) – 2.682(6) Å], even though these values remain within the range reported for axial Cu^{II}–O bonds (2.22 – 2.89 Å) [40].

One hydrogen bond is formed with the H atom of the μ_3-OH ligand as a donor and the methanol O(301) atom as an acceptor. A second hydrogen bond involves the H of the hydroxyl group form the methanol molecule ~~as donor~~ and the perchlorate O(203) ~~as acceptor~~. The most relevant hydrogen bond parameters are listed in Table 3. These hydrogen bonds result in pseudo-dimeric aggregates of triangular fragments linked through two solvate molecules (see Figure S1 in the Supporting Information). Lastly, the shortest intermolecular Cu···Cu distance is 6.173(2) Å between Cu(1) and Cu(2*i*) with *i* = – *x*, ½ + *y*, ½ – *z*.

~~Compound **2** crystallizes in the monoclinic space group Pn. The structure consists of neutral zig-zag chains of six-coordinated copper ions, aligned along the *b* direction. [Something here should be said about six different crystallographic copper sites?] The Cu^{II} ions show a rather distorted octahedral geometry, being bonded to four N atoms from one mpko$^-$ ion and one neutral mpkoH molecule in equatorial positions. Axial sites are occupied by one O atom from a perchlorate ion and one O atom from the mpko$^-$ ion chelated to a neighbour metal center in the chain. This way, the mpko$^-$ ions bridge pairs of copper atoms also in 2.111 mode. However, in this case the Cu–N–O–Cu dihedral angles average 114(2)° resulting in *anti* conformation. Equatorial Cu–N and axial Cu–O distances range from 1.884(18) to 2.157(18) Å, and from 2.459(14) to 2.763(15) Å, respectively. In turn, dihedral angles between mean equatorial planes at adjacent copper sites on the chain range from 47.2(4) to 60.8(4)° (Figure S2). The intrachain Cu···Cu average distance through the oximato bridge is 5.25(14) Å, while the shortest interchain Cu···Cu distance is 9.0673(37) Å between Cu(1) and Cu(6*ii*) with *ii* = – ½ + *x*, 1 – *y*, ½ + *z*.~~

Compound **3** crystallizes in the orthorhombic space group Pnma, and its structure can be described as composed of {Cu[$(mpko)_2BF_2$](H_2O)}$^+$ cations and BF_4^- anions. The copper atom is five-coordinated, the tetradentate $(mpko)_2BF_2^-$ ligand defining the equatorial plane and one H_2O molecule in apical position building a square pyramidal complex. The shortest intermolecular Cu···Cu distance is 7.6474(14) Å between Cu(1) and Cu(1*iii*) with *iii* = *x*, *y*, 1 + *z*.

3.3. Magnetic Properties

In this section, we discuss in detail the magnetic properties of compounds **1** and **2**. Data for complex **3** are given in the supplementary material.

The magnetic properties of **1** in the form of $\chi_M T$ versus T plot are shown in Figure 4, χ_M being the molar magnetic susceptibility per Cu_3 trinuclear unit. At room temperature, $\chi_M T$ is 0.49 cm^3 K mol^{-1}, a value that is lower than expected for three magnetically isolated Cu^{II} ions ($\chi_M T \approx 1.2$ cm^3 K mol^{-1} for S = ½ and g_{Cu} = 2.1), indicating the presence of significant antiferromagnetic interactions. Upon cooling, the curve decreases continuously. Between 200 and 70 K approximately, the $\chi_M T$ values decline slowly, from 0.43 to 0.39 cm^3 K mol^{-1}, close to the expected value for an isolated S = ½ ground state ($\chi_M T \approx 0.41$ cm^3 K mol^{-1} with g = 2.1). On further cooling, the curve decreases rapidly to reach a value of 0.23 cm^3 K mol^{-1} at 2.0 K.

This behavior has been previously observed in triangular tricopper(II) complexes and has been thoroughly explained recently in terms of a relatively large antisymmetric exchange, which is responsible for the low-temperature $\chi_M T$ values being much lower than expected for an isotropic system [31,41,42].

Then, the appropriate phenomenological spin Hamiltonian, taking also into account the Zeeman perturbation in axially distorted surroundings, is given by Eq. 4:

$$\hat{H} = \hat{H}_{\mathrm{iso}} + \hat{H}_{\mathrm{ase}} + \hat{H}_{\mathrm{Zee}}$$

where $\hat{H}_{\mathrm{iso}}$ is the isotropic Heisenberg-Dirac-Van Vleck Hamiltonian applied to a triangle of spin doublets S_1, S_2 and S_3, $\hat{H}_{\mathrm{ase}}$ corresponds to the antisymmetric exchange interaction, and $\hat{H}_{\mathrm{Zee}}$ describes the Zeeman interactions, as:

$$\hat{H}_{\mathrm{iso}} = -J_{12}\,\hat{S}_1\cdot\hat{S}_2 - J_{23}\,\hat{S}_2\cdot\hat{S}_3 - J_{31}\,\hat{S}_3\cdot\hat{S}_1$$

$$\hat{H}_{\mathrm{ase}} = \mathbf{G}_{12}\left[\hat{S}_1\times\hat{S}_2\right] + \mathbf{G}_{23}\left[\hat{S}_2\times\hat{S}_3\right] + \mathbf{G}_{31}\left[\hat{S}_3\times\hat{S}_1\right]$$

$$\hat{H}_{\mathrm{Zee}} = g_{\parallel}\mu_{\mathrm{B}}\left(\hat{S}_{1z}+\hat{S}_{2z}+\hat{S}_{3z}\right)H_z + g_{\perp}\mu_{\mathrm{B}}\left[\left(\hat{S}_{1x}+\hat{S}_{2x}+\hat{S}_{3x}\right)H_x + \left(\hat{S}_{1y}+\hat{S}_{2y}+\hat{S}_{3y}\right)H_y\right]$$

In these expressions, J_{ij} and $\mathbf{G}_{\mathrm{ij}}$ are the isotropic exchange constants and the antisymmetric vectors, respectively, between copper atoms *i* and *j*, $\hat{S}_{\mathrm{i}}$ and $\hat{S}_{\mathrm{i}u}$ (with u = x, y, z) are the corresponding spin operators for the *i*-th center, H_u are the components of the magnetic field, $g_{\parallel}$ and $g_{\perp}$ are the components of the g tensor in the parallel (z) and perpendicular (x, y) directions and μ_{B} is the Bohr magneton.

Clearly, it is impossible to determinate unambiguously the large number of parameters involved in these Hamiltonians, which requires to propose a more simplified model based on some reasonable approximations. In fact, a first approximation has already been done implicitly, assuming an axial Zeeman interaction and identical g values for the three Cu^{II} ions. Secondly, the complex **1** can be considered as an isosceles triangle, with penta-coordinated Cu(1) and Cu(2) treated as equivalent, that is $J = J_{13} = J_{23} \neq J_{12} = j$. An equilateral triangle would require only one isotropic exchange constant J, but in practice this approximation usually fails. Equilateral triangles distort to isosceles ones due to the Jahn-Teller effect, and the isotropic exchange turns out to be sensitive to these distortions, in particular at low temperatures.

On the other hand, in an isosceles triangle, the components of the three $\mathbf{G}_{\mathrm{ij}}$ vectors must satisfy the condition $\mathbf{G}_{13}{}^{u} = \mathbf{G}_{23}{}^{u} \neq \mathbf{G}_{12}{}^{u}$ (u = x, y, z), which would mean six different parameters to be determined. At this point we can assume that even if the three $Cu^{II}\cdots Cu^{II}$ pairs are structurally non-equivalent, the expected differences between the corresponding vectors will not be significant and so we may suppose $\mathbf{G}_{13}{}^{u} = \mathbf{G}_{23}{}^{u} \approx \mathbf{G}_{12}{}^{u}$. Then, there would be only three parameters, G_{X}, G_{Y} and G_{Z}. Nevertheless, it has been previously found that in these kind of trinuclear copper complexes G_{X} and G_{Y} are very small compared to G_{Z} so they could be neglected. In fact, this approach is equivalent to assume that the triangle behaves as equilateral as far as ASE is considered, since according to Moriya, the condition $G_{\mathrm{X}} = G_{\mathrm{Y}} = 0$ and G_{Z} being the only ASE parameter would only be strictly valid in D_{3h} symmetry, with G_{Z} parallel to the C_3 axis.

With all these considerations, an analytical expression for the magnetic susceptibility in the low-field limit ($H \ll \Delta$) is given by Eq. 5 [42]:

$$\chi_{\mathrm{M}}^{\parallel} = \frac{N\mu_{\mathrm{B}}{}^{2}g_{\parallel}{}^{2}}{4kT}\left[\frac{\cosh(x) + 5\exp(3J_{\mathrm{av}}/2kT)}{\cosh(x) + \exp(3J_{\mathrm{av}}/2kT)}\right]$$

$$\chi_{\mathrm{M}}^{\perp} = \frac{N\mu_{\mathrm{B}}{}^{2}g_{\perp}{}^{2}}{4kT}\left[\frac{\rho^{2}\cosh(x) + 5\exp(3J_{\mathrm{av}}/2kT) + (1-\rho^{2})\sinh(x)/x}{\cosh(x) + \exp(3J_{\mathrm{av}}/2kT)}\right]$$

$$\chi_{\mathrm{M}}^{\mathrm{av}} = \left(\chi_{\mathrm{M}}^{\parallel} + 2\chi_{\mathrm{M}}^{\perp}\right)/3$$

where N is the Avogadro number, k is the Boltzmann constant, $J_{\mathrm{av}} = (2J + j)/3$, $x = \Delta/2kT$ and $\rho = \delta/\Delta$, with $\delta = J - j$ and $\Delta = \left(\delta^{2} + 3G_{\mathrm{Z}}{}^{2}\right)^{1/2}$.

The best least-squares fit parameters are then J_{av} = –441(2) cm^{-1}, δ = 40(3) cm^{-1}, G_{Z} = 39.7(7) cm^{-1}, $g_{\parallel}$ = 2.25(4) and $g_{\perp}$ = 2.03(2), with R = 1.90 × 10^{-5} (R is the agreement factor defined as $\Sigma i[(\chi_{M}T)_{obs}(i) - (\chi_{M}T)_{calcd}(i)]^{2}/\Sigma i[(\chi_{M}T)_{obs}(i)]^{2}$), although the values of $g_{\parallel}$ and $g_{\perp}$ are highly correlated. Alternatively, if $g_{\perp}$ is fixed at 2.0, the best-fit parameters are J_{av} = –442 cm^{-1}, δ = 38 cm^{-1}, G_{Z} = 40.3 cm^{-1} and $g_{\parallel}$ = 2.304(1), with R = 1.94 × 10^{-5}. The calculated curve reproduces remarkably well the experimental magnetic data in the whole temperature range.

The X-band EPR spectrum of **1** at 4.5 K displays two bands (Figure 5). The first one near 3.0 kG corresponds to $g_{\parallel}$ = 2.26, which is a typical average value for Cu^{II} ions in axial symmetry. The second band at higher field can be assigned to an effective $g'_{\perp}$ value of 0.75. This transition with $g'_{\perp} \ll g_{e}$ is normally found for Cu_3 triangles in which antisymmetric exchange is important

[41]. In weakly axial systems ($|J_{av}| \gg \delta$) $g'_\perp$ can be related to the true average $g_\perp$ value of the local Cu^{II} ions according to Eq. 6:

$$g'_\perp \approx g_\perp \frac{\delta}{\Delta}$$

In this case, the $g'_\perp$ value calculated from magnetic susceptibility data is 1.02, which compares reasonable well with the one obtained from the EPR spectrum.

At very low temperature, the only populated state is a ground spin doublet, then the magnetization curves for **1** at different temperatures were fitted by a Brillouin function for an $S = ½$ with g = 1.48 (Figure 6). Using Eq. 7 with the experimental EPR values for $g_\parallel$ and $g'_\perp$:

$$g_{av}{}^2 = \left(g_\parallel{}^2 + 2\, g'_\perp{}^2\right)/3$$

a value of g_{av} = 1.40 can be calculated, which is in agreement with the g obtained from magnetization measurements.

The magnetic properties of **2** in the form of $\chi_M T$ versus T plot are shown in Figure 7, χ_M being the molar magnetic susceptibility per Cu^{II} ion. At room temperature, $\chi_M T$ is 0.44 cm^3 K mol^{-1}, a value slightly higher than expected for one magnetically isolated Cu^{II} ion. Upon cooling, the $\chi_M T$ values remain rather constant until 40 K and then rise up to reach a value of 0.62 cm^3 K mol^{-1} at 2.0 K, indicating the presence of ferromagnetic interactions.

~~Having in mind the minor differences between distinct copper sites in **2**,~~ the magnetic data can be described by the spin Hamiltonian of Eq. 8, which considers the isotropic interaction between equivalent nearest neighbor Cu^{II} ions in a regular chain:

$$\hat{H} = -J \sum_{i=1}^{n-1} \hat{S}_{\mathrm{Cu}_i} \cdot \hat{S}_{\mathrm{Cu}_{i+1}}$$

When n tends to infinite, there is no analytical expression for the magnetic susceptibility, but the experimental data can be fitted by the numerical expression of Eq. 9 [43,44]:

$$\chi = \frac{N\mu_B{}^2 g^2}{4kT}\left[\frac{1.0 + 5.798y + 16.903y^2 + 29.377y^3 + 29.833y^4 + 14.037y^5}{1.0 + 2.798y + 7.009y^2 + 8.654y^3 + 4.574y^4}\right]$$

with

$$y = \frac{J}{2kT}$$

In this case, the best-fit parameters are J = +0.73(5) cm^{-1} and g = 2.14(1), with R = 1.7×10^{-4}. The calculated curve reproduces very well the experimental data in the whole temperature range. In turn, a similar average g value of 2.11 is obtained from EPR measurements ($g_\parallel$ = 2.17 and $g_\perp$ = 2.08, Figure S3).

4. Concluding remarks

Two new Cu^{II} complexes with mpkoH have been prepared by reaction of $Cu(ClO_4)_2$ with the oxime in CH_3OH. Depending on the metal-to-ligand reaction ratio, the trinuclear complex $[Cu_3(OH)(ClO_4)_2(mpko)_3]\cdot CH_3OH$ or the chain $[Cu(ClO_4)(mpko)(mpkoH)]_n$ can be obtained.

The geometrically spin-frustrated triangular $[Cu^{II}_3]$ core in **1** exhibits strong antiferromagnetic coupling (J_{av} = –441 cm^{-1}, δ = 40 cm^{-1}) and antisymmetric exchange (G_Z = 40 cm^{-1}). The magnetic interaction between the Cu^{II} ions within the triangle is mediated by both the oxime and the hydroxo bridges. Nevertheless, it has been previously found that the main structural factor that determine the nature and magnitude of the isotropic magnetic coupling (J) in $\{Cu_3(\mu_3\text{-}X)L_3\}^{2+}$ cores is the Cu–X–Cu angle (θ). Magnetostructural correlations have been proposed, based on both theoretical studies and empirical data, showing that the closer the Cu–X–Cu angles to 120°, the stronger the antiferromagnetic interaction. However, the number of studied cases is small, and different linear equations relating J and θ have been suggested for X = OH and L = oxime.

Our results in J_{av} (and δ) are in good agreement with data found in other oximate-bridged Cu_3 triangles, and with estimated values from proposed correlation equations. Also the antisymmetric exchange parameter G_Z value is in agreement with the results reported for analogous compounds, as seen in Table 6.

The average magnetic coupling between the Cu^{II} ions through the oximato bridge in **2** is very weak. This can be understood qualitatively through orbital symmetry considerations. A good overlap between magnetic orbitals in neighbor centers favors strong antiferromagnetic interaction, while strict orthogonality leads to ferromagnetic coupling. A representative Cu···Cu structural fragment of **2** and the corresponding pictures of the magnetic orbitals delocalized toward the bridge are shown in Scheme 2. Given the tetragonal elongated octahedral coordination of the Cu(1) and Cu(2), the magnetic orbital in both metal ions is the dx2-y2 type-orbital. Due to the fact that dihedral angles between mean equatorial planes at adjacent copper sites are relatively high, the magnetic orbitals centered in Cu(1) and Cu(2) are unfavorably oriented to interact and their resultant overlap should be fairly low.

Acknowledgements

The authors thank the financial support from the Programa de Desarrollo de Ciencias Básicas (Uruguay), the Ministerio Español de Economía y Competitividad (Project CTQ2013-44844P) and the Generalitat Valenciana (PROMETEOII/2014-070) (Spain), ~~the Ministero dell'Istruzione, dell'Università e della Ricerca (Italy)~~. L.M. is indebted to the ANII for a grant (Uruguay).

Appendix A. Supplementary material

CCDC xxxxxxx (**1**), yyyyyyy (**2**) and 1538260 (**3**) contain the supplementary crystallographic data for this paper. These data can be obtained free of charge from The Cambridge Crystallographic Data Centre via www.ccdc.cam.ac.uk/data_request/cif. Supplementary data associated with this article can be found, in the online version, at doi:xx.xxxx/................

References

[1] R.B. Singh, B.S. Garg, R.P. Singh, Oximes as spectrophotometric reagents—a review, Talanta. 26 (1979) 425–444. doi:10.1016/0039-9140(79)80107-1.

[2] C.J. Milios, T.C. Stamatatos, S.P. Perlepes, The coordination chemistry of pyridyl oximes, Polyhedron. 25 (2006) 134–194. doi:10.1016/j.poly.2005.07.022.

[3] T.C. Stamatatos, D. Foguet-Albiol, C.C. Stoumpos, C.P. Raptopoulou, A. Terzis, W. Wernsdorfer, S.P. Perlepes, G. Christou, New Mn3 structural motifs in manganese single-molecule magnetism from the use of 2-pyridyloximate ligands, Polyhedron. 26 (2007) 2165–2168. doi:10.1016/j.poly.2006.10.025.

[4] T.C. Stamatatos, G. Christou, Azide Groups in Higher Oxidation State Manganese Cluster Chemistry: From Structural Aesthetics to Single-Molecule Magnets, Inorg. Chem. 48 (2009) 3308–3322. doi:10.1021/ic801217j.

[5] C.C. Stoumpos, T.C. Stamatatos, H. Sartzi, O. Roubeau, A.J. Tasiopoulos, V. Nastopoulos, S.J. Teat, G. Christou, S.P. Perlepes, Employment of methyl 2-pyridyl ketone oxime in manganese non-carboxylate chemistry: MnII2MnIV and MnII2MnIII6 complexes, Dalton Trans. (2009) 1004–1015. doi:10.1039/B813828A.

[6] D.I. Alexandropoulos, C. Papatriantafyllopoulou, G. Aromí, O. Roubeau, S.J. Teat, S.P. Perlepes, G. Christou, T.C. Stamatatos, The Highest-Nuclearity Manganese/Oximate Complex: An Unusual MnII/III15 Cluster with an S = 6 Ground State, Inorg. Chem. 49 (2010) 3962–3964. doi:10.1021/ic100267y.

[7] C.C. Stoumpos, R. Inglis, O. Roubeau, H. Sartzi, A.A. Kitos, C.J. Milios, G. Aromí, A.J. Tasiopoulos, V. Nastopoulos, E.K. Brechin, S.P. Perlepes, Rare Oxidation-State Combinations and Unusual Structural Motifs in Hexanuclear Mn Complexes Using 2-Pyridyloximate Ligands, Inorg. Chem. 49 (2010) 4388–4390. doi:10.1021/ic100089y.

[8] S. Zhang, L. Zhen, B. Xu, R. Inglis, K. Li, W. Chen, Y. Zhang, K.F. Konidaris, S.P. Perlepes, E.K. Brechin, Y. Li, Wheel-like MnII6 and NiII6 complexes from the use of 2-pyridinealdoxime and carboxylates, Dalton Trans. 39 (2010) 3563–3571. doi:10.1039/B922672A.

[9] C. Papatriantafyllopoulou, T.C. Stamatatos, W. Wernsdorfer, S.J. Teat, A.J. Tasiopoulos, A. Escuer, S.P. Perlepes, Combining Azide, Carboxylate, and 2-Pyridyloximate Ligands in Transition-Metal Chemistry: Ferromagnetic NiII5 Clusters with a Bowtie Skeleton, Inorg. Chem. 49 (2010) 10486–10496. doi:10.1021/ic1014829.

[10] T.C. Stamatatos, K.A. Abboud, S.P. Perlepes, G. Christou, The highest nuclearity metal oxime clusters: Ni14 and Ni12Na2 complexes from the use of 2-pyridinealdoximate and azide ligands, Dalton Trans. (2007) 3861–3863. doi:10.1039/B708189H.

[11] C.G. Efthymiou, A.A. Kitos, C.P. Raptopoulou, S.P. Perlepes, A. Escuer, C. Papatriantafyllopoulou, Employment of the sulfate ligand in 3d-metal cluster chemistry: A novel hexanuclear nickel(II) complex with a chair metal topology, Polyhedron. 28 (2009) 3177–3184. doi:10.1016/j.poly.2009.04.015.

[12] J. Esteban, L. Alcázar, M. Torres-Molina, M. Monfort, M. Font-Bardia, A. Escuer, High Nuclearity in Azido/Oximate Chemistry: Ni14 and Ni13 Clusters with S = 6 and 9 Ground States, Inorg. Chem. 51 (2012) 5503–5505. doi:10.1021/ic3004036.

[13] A. Escuer, J. Mayans, M. Font-Bardia, Linked Nickel Metallacrowns from a Phosphonate/2-Pyridyloximate Blend of Ligands: Structure and Magnetic Properties, Inorg. Chem. 55 (2016) 3161–3168. doi:10.1021/acs.inorgchem.6b00103.

[14] T.C. Stamatatos, C. Papatriantafyllopoulou, E. Katsoulakou, C.P. Raptopoulou, S.P. Perlepes, 2-Pyridyloximate clusters of cobalt and nickel, Polyhedron. 26 (2007) 1830–1834. doi:10.1016/j.poly.2006.09.060.

[15] C.D. Polyzou, H. Nikolaou, C. Papatriantafyllopoulou, V. Psycharis, A. Terzis, C.P. Raptopoulou, A. Escuer, S.P. Perlepes, Employment of methyl 2-pyridyl ketone oxime in 3d/4f-metal chemistry: dinuclear nickel(II)/lanthanide(III) species and complexes containing the metals in separate ions, Dalton Trans. 41 (2012) 13755–13764. doi:10.1039/C2DT31928D.

[16] T.C. Stamatatos, D. Foguet-Albiol, S.-C. Lee, C.C. Stoumpos, C.P. Raptopoulou, A. Terzis, W. Wernsdorfer, S.O. Hill, S.P. Perlepes, G. Christou, “Switching On” the Properties of Single-Molecule Magnetism in Triangular Manganese(III) Complexes, J. Am. Chem. Soc. 129 (2007) 9484–9499. doi:10.1021/ja072194p.

[17] C. Papatriantafyllopoulou, T.C. Stamatatos, C.G. Efthymiou, L. Cunha-Silva, F.A.A. Paz, S.P. Perlepes, G. Christou, A High-Nuclearity 3d/4f Metal Oxime Cluster: An Unusual Ni8Dy8 “Core−Shell” Complex from the Use of 2-Pyridinealdoxime, Inorg. Chem. 49 (2010) 9743–9745. doi:10.1021/ic101581g.

[18] R. Clérac, H. Miyasaka, M. Yamashita, C. Coulon, Evidence for Single-Chain Magnet Behavior in a MnIII−NiII Chain Designed with High Spin Magnetic Units: A Route to High Temperature Metastable Magnets, J. Am. Chem. Soc. 124 (2002) 12837–12844. doi:10.1021/ja0203115.

[19] R. Beckett, B.F. Hoskins, Crystal and molecular structure of a trinuclear copper(II) complex: μ3-hydroxo-tri-μ-(pyridine-2-carbaldehyde oximato)-μ3-sulphato-tricopper(II)–16·3water, J. Chem. Soc. Dalton Trans. (1972) 291–295. doi:10.1039/DT9720000291.

[20] E.O. Schlemper, J. Stunkel, C. Patterson, Structure of dinuclear bis(di-2-pyridylmethanone oximato)copper(II) dihydrate, Acta Crystallogr. Sect. C. 46 (1990) 1226–1228.

[21] P. Chaudhuri, M. Winter, U. Flörke, H.-J. Haupt, An effectively diamagnetic oximato-bridged asymmetric dinuclear copper(II) complex with a Cu(II)�I bond, Inorganica Chim. Acta. 232 (1995) 125–130. doi:10.1016/0020-1693(94)04379-A.

[22] T.C. Stamatatos, J.C. Vlahopoulou, Y. Sanakis, C.P. Raptopoulou, V. Psycharis, A.K. Boudalis, S.P. Perlepes, Formation of the core in copper(II) carboxylate chemistry via use of di-2-pyridyl ketone oxime [(py)2CNOH] : [Cu3(OH)(O2CR)2{(py)2CNO}3] (R = Me, Ph), Inorg. Chem. Commun. 9 (2006) 814–818. doi:10.1016/j.inoche.2006.04.032.

[23] T. Afrati, C. Dendrinou-Samara, C. Raptopoulou, A. Terzis, V. Tangoulis, D.P. Kessissoglou, Copper inverse-9-metallacrown-3 compounds showing antisymmetric magnetic behaviour, Dalton Trans. (2007) 5156–5164. doi:10.1039/B708767E.

[24] T. Afrati, C. Dendrinou-Samara, C. Raptopoulou, A. Terzis, V. Tangoulis, A. Tsipis, D.P. Kessissoglou, Experimental and Theoretical Study of the Antisymmetric Magnetic Behavior of Copper inverse-9-Metallacrown-3 Compounds, Inorg. Chem. 47 (2008) 7545–7555. doi:10.1021/ic8003257.

[25] T. Afrati, A.A. Pantazaki, C. Dendrinou-Samara, C. Raptopoulou, A. Terzis, D.P. Kessissoglou, Copper inverse-9-metallacrown-3 compounds interacting with DNA, Dalton Trans. 39 (2009) 765–775. doi:10.1039/B914112J.

[26] E.S. Koumousi, C.P. Raptopoulou, S.P. Perlepes, A. Escuer, T.C. Stamatatos, Strong antiferromagnetic coupling in doubly N,O oximato-bridged dinuclear copper(II) complexes, Polyhedron. 29 (2010) 204–211. doi:10.1016/j.poly.2009.07.010.
[27] G.-X. Liu, W. Guo, S. Nishihara, X.-M. Ren, A chiral copper(II) inverse-9-metallacrown-3 complex: Synthesis, crystal structure, ferroelectric and magnetic properties, Inorganica Chim. Acta. 368 (2011) 165–169. doi:10.1016/j.ica.2010.12.067.
[28] R. Li, J. Lu, D. Li, S. Cheng, J. Dou, Syntheses, structures, in vitro cytotoxicities and DNA-binding properties of four copper complexes based on a phenyl 2-pyridyl ketoxime ligand, Transit. Met. Chem. 39 (2014) 507–517. doi:10.1007/s11243-014-9826-9.
[29] M. Hołyńska, Structural variety and magnetic properties of oxime-bridged copper(II) complexes, J. Mol. Struct. 1098 (2015) 175–180. doi:10.1016/j.molstruc.2015.06.014.
[30] A. Tarushi, C.P. Raptopoulou, V. Psycharis, C.K. Kontos, D.P. Kessissoglou, A. Scorilas, V. Tangoulis, G. Psomas, Copper(II) Inverse-[9-Metallacrown-3] Compounds Accommodating -Nitrato or Diclofenac Ligands: Structure, Magnetism, and Biological Activity, Eur. J. Inorg. Chem. 2016 (2016) 219–231. doi:10.1002/ejic.201500769.
[31] A. Escuer, G. Vlahopoulou, F. Lloret, F.A. Mautner, Spin Frustration in Triangular Cu3II Complexes with 6-Methyl-2-pyridyloxime as Ligand – Synthesis, Structural, and Magnetic Characterization, Eur. J. Inorg. Chem. 2014 (2014) 83–92. doi:10.1002/ejic.201300910.
[32] S. Speed, M. Font-Bardía, M.S.E. Fallah, R. Vicente, Four new trinuclear {Cu3(μ3-OH)(oximate)3}2+ clusters: crystal structure and magnetic behaviour, Dalton Trans. 43 (2014) 16919–16927. doi:10.1039/C4DT02215G.
[33] R.H. Holm, E.I. Solomon, Preface: Biomimetic Inorganic Chemistry, Chem. Rev. 104 (2004) 347–348. doi:10.1021/cr0206364.
[34] A. Chakraborty, K.L. Gurunatha, A. Muthulakshmi, S. Dutta, S.K. Pati, T.K. Maji, Assembly of trinuclear and tetranuclear building units of Cu2+ towards two 1D magnetic systems: synthesis and magneto-structural correlations, Dalton Trans. 41 (2012) 5879–5888. doi:10.1039/C2DT12511K.
[35] L. Croitor, E.B. Coropceanu, O. Petuhov, K.W. Krämer, S.G. Baca, S.-X. Liu, S. Decurtins, M.S. Fonari, A one-dimensional coordination polymer based on Cu3-oximato metallacrowns bridged by benzene-1,4-dicarboxylato ligands: structure and magnetic properties, Dalton Trans. 44 (2015) 7896–7902. doi:10.1039/C5DT00533G.
[36] X. Qiu, L. Li, D. Li, Chlorido[1-(pyridin-2-yl)ethanone oximato-[kappa]2N,N'][1-(2-pyridyl)ethanone oxime-[kappa]2N,N']copper(II) trihydrate, Acta Crystallogr. Sect. E. 67 (2011) m1810–m1811.
[37] B. Zhong, S. Li, G. Chen, Aqua[1-(pyridin-2-yl)ethanone oximato][1-(2-pyridin-2-yl)ethanone oxime]copper(II) perchlorate monohydrate, Acta Crystallogr. Sect. E. 68 (2012) m874.
[38] P. Chaudhuri, T. Weyhermüller, R. Wagner, S. Khanra, B. Biswas, E. Bothe, E. Bill, Tridentate Facial Ligation of Tris(pyridine-2-aldoximato)nickel(II) and Tris(imidazole-2-aldoximato)nickel(II) To Generate NiIIFeIIINiII, MnIIINiII, NiIINiII, and ZnIINiII and the Electrooxidized MnIVNiII, NiIINiIII, and ZnIINiIII Species: A Magnetostructural, Electrochemical, and EPR Spectroscopic Study, Inorg. Chem. 46 (2007) 9003–9016. doi:10.1021/ic701073j.
[39] R.A. Coxall, S.G. Harris, D.K. Henderson, S. Parsons, P.A. Tasker, R.E.P. Winpenny, Inter-ligand reactions: in situ formation of new polydentate ligands, J Chem Soc Dalton Trans. (2000) 2349–2356. doi:10.1039/B001404O.
[40] G. Wilkinson, R.D. Gillard, J.A. McCleverty, Comprehensive Coordination Chemistry: Late transition elements, Pergamon Press, 1987. https://books.google.com.uy/books?id=DHQ6AQAAIAAJ.
[41] X. Liu, M.P. de Miranda, E.J.L. McInnes, C.A. Kilner, M.A. Halcrow, Antisymmetric exchange in two tricopper(II) complexes containing a [Cu3(μ3-OMe)]5+ core, Dalton Trans. (2004) 59–64. doi:10.1039/B311980G.

[42] S. Ferrer, F. Lloret, E. Pardo, J.M. Clemente-Juan, M. Liu-González, S. García-Granda, Antisymmetric Exchange in Triangular Tricopper(II) Complexes: Correlation among Structural, Magnetic, and Electron Paramagnetic Resonance Parameters, Inorg. Chem. 51 (2012) 985–1001. doi:10.1021/ic2020034.
[43] O. Kahn, Molecular magnetism, VCH, 1993. https://books.google.com.uy/books?id=QwzwAAAAMAAJ.
[44] G.A. Baker, G.S. Rushbrooke, H.E. Gilbert, High-Temperature Series Expansions for the Spin-\textonehalf{} Heisenberg Model by the Method of Irreducible Representations of the Symmetric Group, Phys. Rev. 135 (1964) A1272–A1277. doi:10.1103/PhysRev.135.A1272.

Figure captions:

Fig. 1. Perpective drawing of the trinuclear unit $[Cu_3(OH)(ClO_4)_2(mpko)_3]$ in (**1**), showing the most relevant atom numbering. Hydrogen atoms were omitted for clarity. Color code: Cu purple, Cl green, O red, N blue, C gray (For interpretation of the references to color in this figure legend, the reader is referred to the web version of this article)

Fig. 2. Partial perspective drawing of the chain structure of $[Cu(ClO_4)(mpko)(mpkoH)]_n$ (**2**), showing the most relevant atom numbering. Color code: Cu purple, Cl green, O red, N blue, C gray

Fig. 3. Structure of the cation $\{Cu[(mpko)_2BF_2](H_2O)\}^+$ in **3**, where most of the hydrogen atoms were omitted for clarity. Color code: Cu purple, B brown, F yellow, O red, N blue, C gray

Fig. 4. Thermal dependence of $\chi_M T$ for compound **1**. The solid line corresponds to the best fit (see the text for details)

Fig. 5. X-Band EPR spectrum of a powdered sample of **1**, recorded at 4.5 K

Fig. 6. Magnetization plots for 1 at 1.9 (triangles), 3 (empty circles) and 4 K (solid circles). The solid lines correspond to the best fits obtained with the Brillouin function for an S = ½ ground state

Fig. 7. Thermal dependence of $\chi_M T$ for compound **2**. The solid line corresponds to the best fit (see the text for details)

Fig. 8. X- band EPR spectrum at 4.5 K of a powder sample of **2**

Scheme captions:

Scheme 1. Coordination modes of mpkoH and the corresponding Harris notation

Scheme 2. Simplified view of a pair of magnetic orbitals centered in two neighbor Cu^{II} ions bridged by $mpko^-$ in **2**

Scheme 1

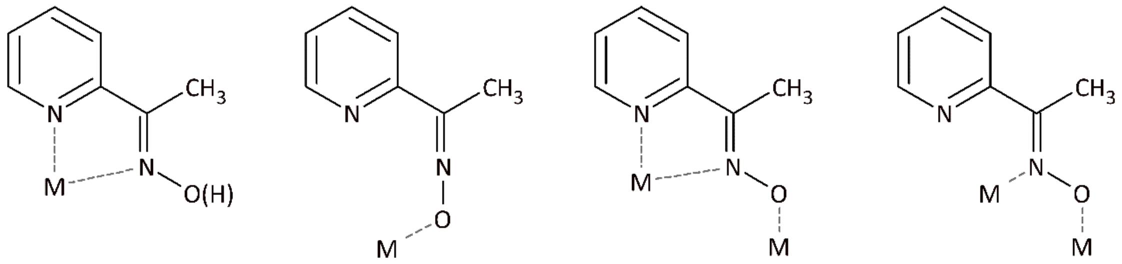

1.011 1.100 2.111 2.110

Scheme 2

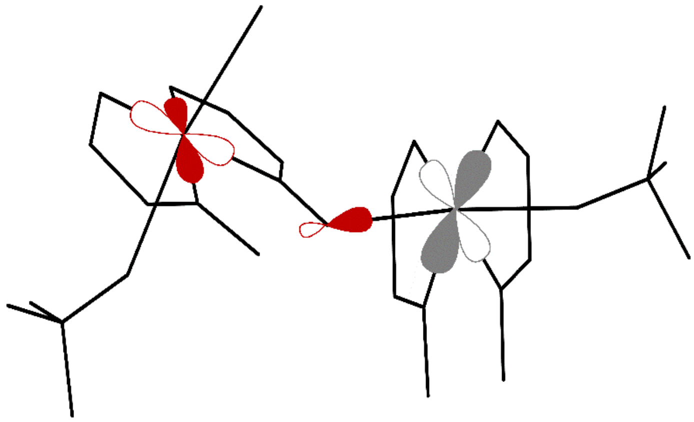

Figure 1

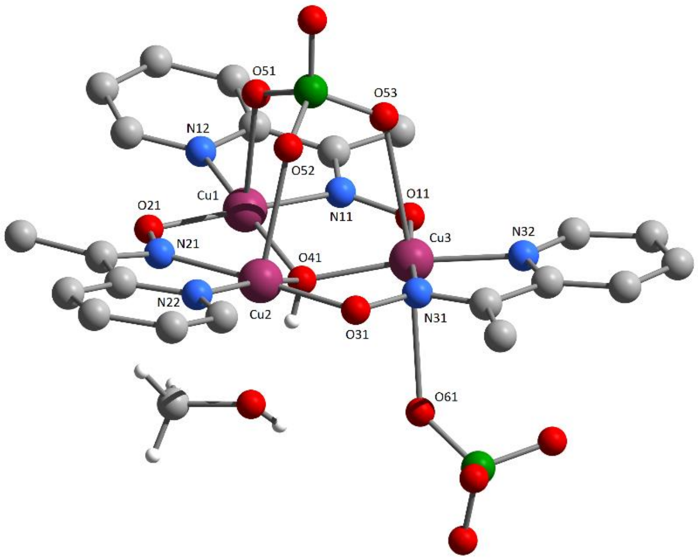

Figure 2 To be removed

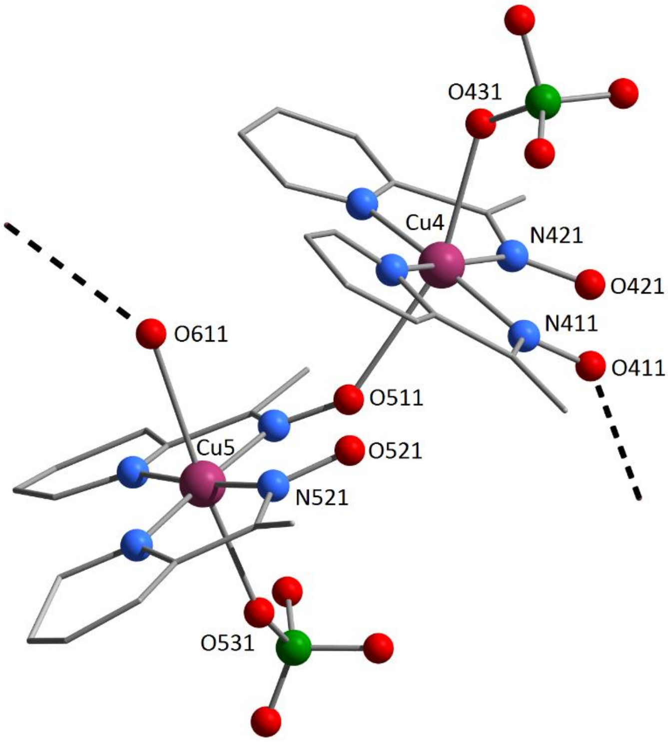

Figure 3

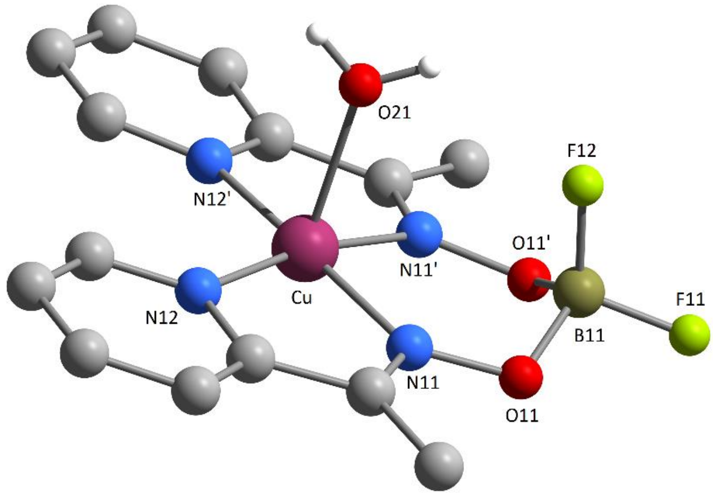

Figure 4

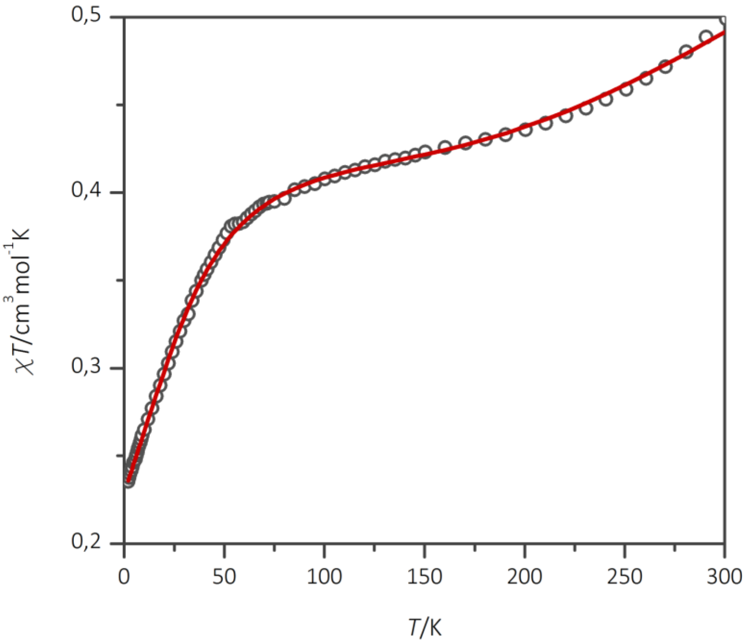

Figure 5

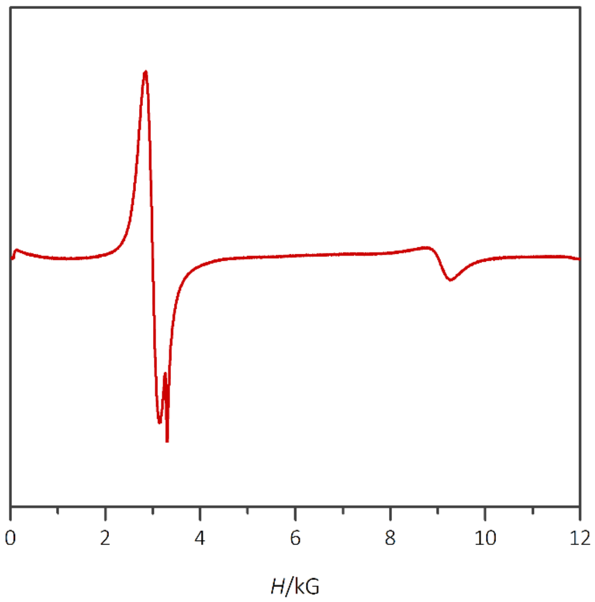

Figure 6

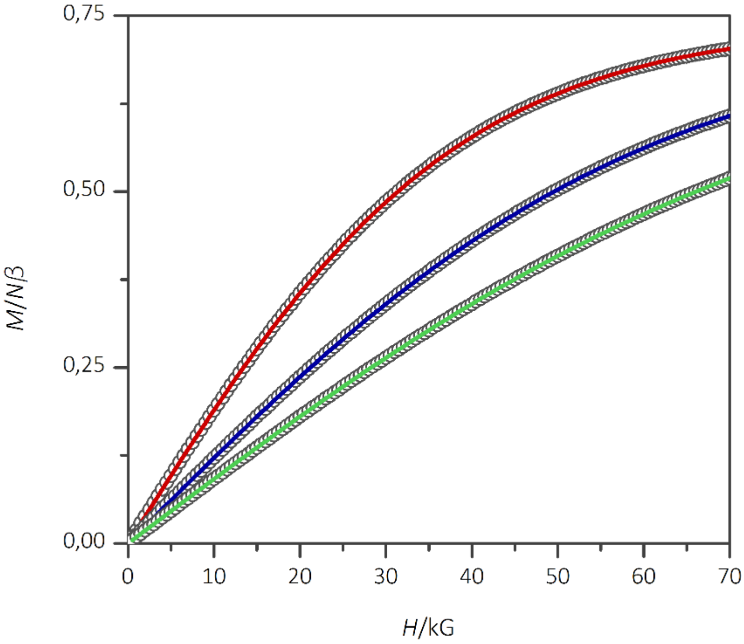

Figure 7

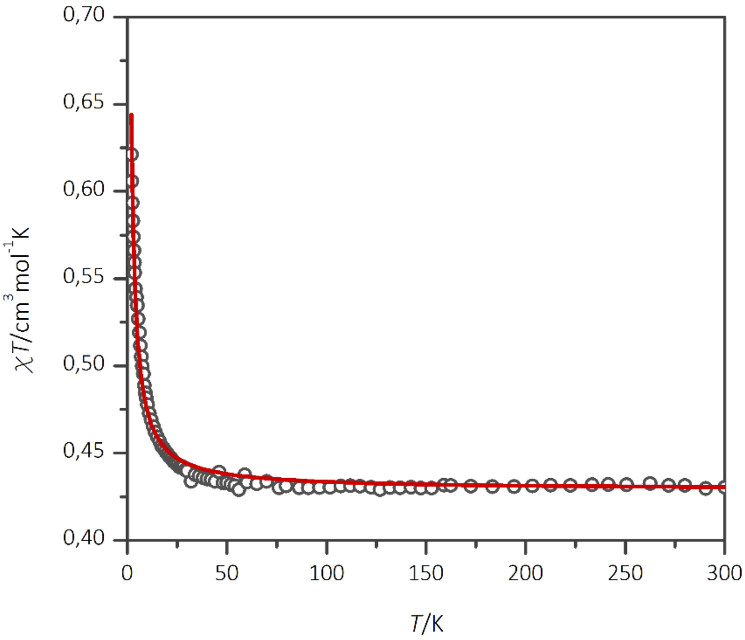
0,70
0,65
0,60
0,55
0,50
0,45
0,40
0
50
100
150
200
250
300
χT/cm³mol⁻¹K
T/K

Supplementary Material

Fig. S1. Pseudo-dimeric aggregates of triangular fragments in **1**, linked by hydrogen bonds through two solvate molecules; mpko^{-} hydrogen and carbon atoms were omitted for clarity. Color code: Cu purple, Cl green, O red, N blue, C gray, H white

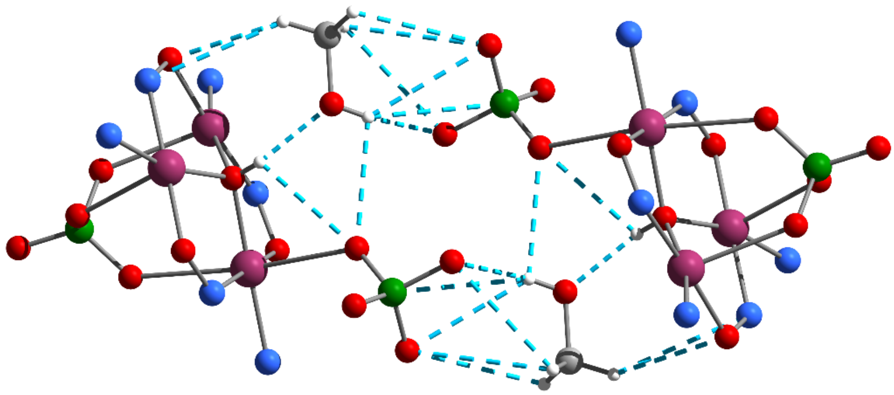

Fig. S2. Simplified view of complex 2, showing the zig-zag chain established by six non-equivalent copper atoms and their coordination environment. Color code: Cu purple, O red, N blue

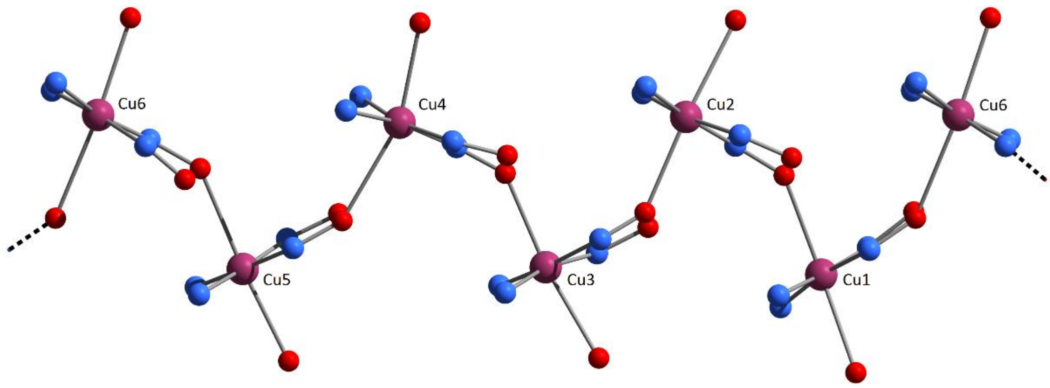

Fig. S3. X-Band EPR spectrum of a powdered sample of **2**, recorded at 4.5 K

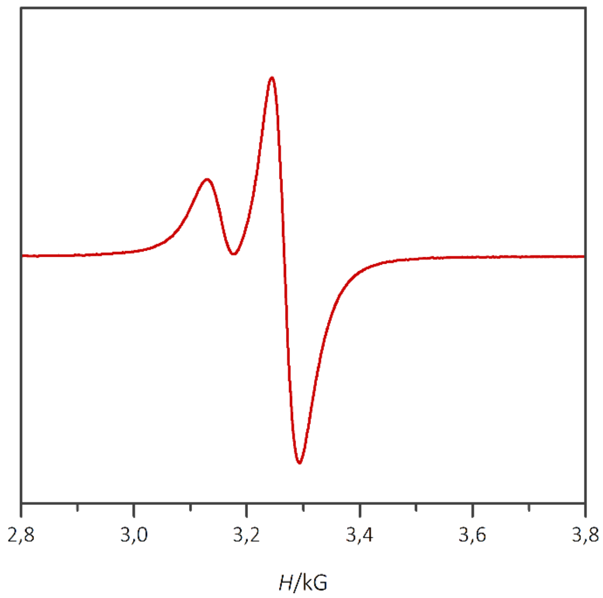

Graphical Abstract

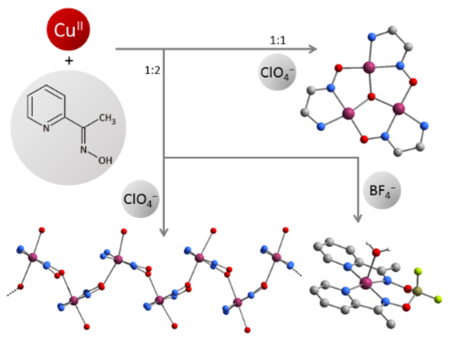

Figure 2 should be moved to supplementary materials and accompanied by the caption below. Numbers in atom labels should be removed (only the numbers).

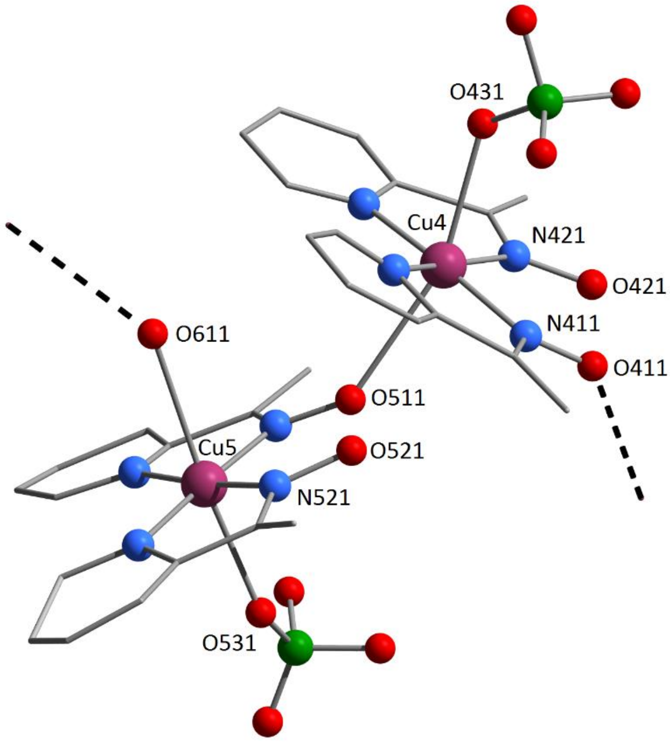

Figure Sx. Proposed structure for [Cu)(μ-mpko)(mpkoH)(ClO_4]$_n$ (**2**). Crystals of **2** were subjected to X-ray diffraction analysis resulting highly pseudosymmetric. Data analysis strongly suggested that they belong to the centrosymmetric space group P21/n. Nevertheless, all the attempts to solve this structure in this space group gave very bad and incomplete models that we were not able to refine. On the other hand, a chemically acceptable model was obtained in the acentric Pn space group. Refinement procedure was difficult, giving a final agreement factor R = 0.15. All attempts to obtain better agreement factors were unsuccessful. However, the obtained model was clear enough to let us rationalize the pseudosymmetric nature of these crystals: while the organic ligands and the copper centers appear to follow all the symmetries required by the P21/n space groups, some of the coordinated perchlorates are disordered and do not admit the inversion symmetry.